



Tide-induced head fluctuations in a confined aquifer with sediment covering its outlet at the sea floor

Hailong Li,^{1,2} Guanyi Li,¹ Jianmei Cheng,² and Michel C. Boufadel³

Received 10 November 2005; revised 28 September 2006; accepted 10 October 2006; published 3 March 2007.

[1] A confined coastal aquifer usually extends under the sea for some distance with its submarine outlet covered by a thin layer of sediment with properties dissimilar from the aquifer. Previous theoretical studies neglected this outlet capping. In this paper an analytical solution is derived for a confined aquifer subject to tidal fluctuations with a leaky boundary condition at the outlet capping. For the cases that offshore length of the aquifer and/or the leakance of the outlet capping are either zero or infinity, existing solutions in literature are obtained. It is shown that our analytical solution can also be used to describe the tidal wave propagation in a confined aquifer extending infinitely under a tidal river. The full solution agreed well with the observations in a piezometer in the Jahe River Basin in China, 200 m inland from the coastline where the tide-induced head fluctuations without delay were observed but cannot be explained using previous analytical and numerical solutions ignoring the effect of the outlet capping. The sensitivity analysis showed that the combined actions of the tidal loading and outlet capping lead to complex dependency of the head fluctuation on the outlet capping's leakance. When the offshore confined aquifer is short, the inland head fluctuation increases with the outlet capping's leakance. In this case significant negative phase shift occurs if the leakance is small. For offshore aquifer length greater than a threshold value the inland head fluctuations are independent of this length and the outlet capping's leakance.

Citation: Li, H., G. Li, J. Cheng, and M. C. Boufadel (2007), Tide-induced head fluctuations in a confined aquifer with sediment covering its outlet at the sea floor, *Water Resour. Res.*, 43, W03404, doi:10.1029/2005WR004724.

1. Introduction

[2] The development in coastal areas requires engineering solutions to ecological and environmental problems such as seawater intrusion, stability of coastal engineering structures, beach dewatering for construction purposes, and deterioration of the marine environment. Although numerical solutions have become standard tools for analyzing such systems [Boufadel, 2000], analytical solutions are still needed because they can reveal the governing parameters of the system, and provide benchmarks for numerical solutions. Analytical studies for tide-induced groundwater flow are numerous. They can be divided into two classes based on aquifer complexity: single aquifer [e.g., Jacob, 1950; Drogue *et al.*, 1984; Sun, 1997; Townley, 1995; Trefry, 1999; Li *et al.*, 2000, 2002] and multilayered aquifer system [e.g., van der Kamp, 1973; Jiao and Tang, 1999; Li *et al.*, 2001; Jeng *et al.*, 2002; Li and Jiao, 2001a, 2001b, 2002a, 2002b, 2003].

[3] Groundwater flow in confined coastal aquifers that extend under the sea has been studied by van der Kamp [1972], Li and Chen [1991a, 1991b], and Li and Jiao [2001a]. In these studies the boundary condition used was

that the subcrop of the aquifer extending under the sea is open on the sea side, and thus directly connected to the sea hydraulically. This condition is not typical, because there is usually a layer of sediment on the sea floor that separates the confined aquifer from the sea [Li and Chen, 1991b]. Such a layer can be modeled as a leaky boundary condition for the groundwater flow in the confined aquifer. Interestingly, such a realistic conceptualization has not been addressed in the literature, and many observed tide-induced groundwater level fluctuations could not be reasonably explained by the existing analytical or even numerical simulations. An example is in the work of Cheng *et al.* [2004], where they could not explain the fluctuations in piezometer GK2A in the Jahe River Basin, Shandong Province, China that was located about 200 m inland from the coastline in a deep confined coastal aquifer. While the analytical solutions and numerical study predictive considerable time lag, observations indicated no delay in the response.

[4] The objective of this paper is to develop a solution for the tide-induced groundwater head fluctuations in a confined coastal aquifer, whose subcrop under the sea is covered with a layer of sediment. The validity of the solution is examined by comparison to field observations from the piezometer GK2A.

2. Mathematical Model and Analytical Solution

2.1. Mathematical Model

[5] Consider a coastal confined aquifer with an impermeable roof that extends under the sea for a distance L . The

¹Department of Mathematics, Anshan Normal University, Anshan, China.

²School of Environmental Studies and Biogeology and Environmental Geology Laboratory, China University of Geosciences, Wuhan, China.

³Department of Civil and Environmental Engineering, Temple University, Philadelphia, Pennsylvania, USA.

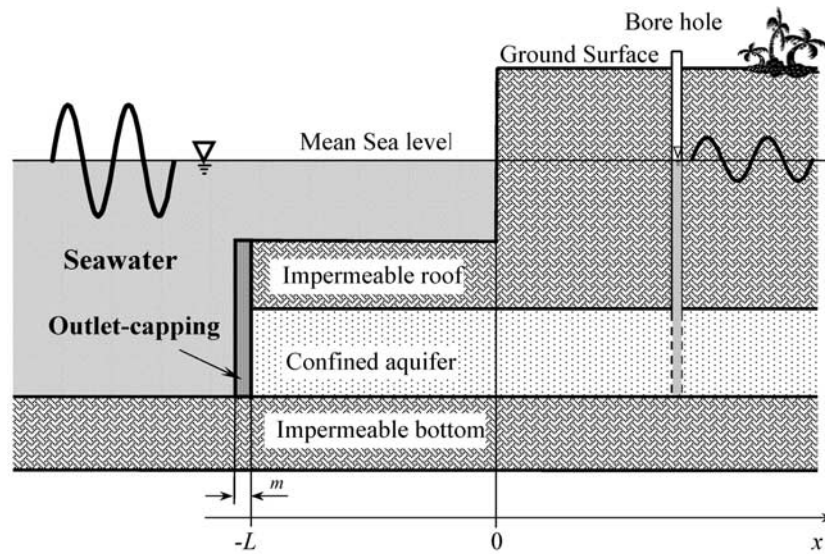


Figure 1. Cross section of a confined aquifer extending under the sea with a thin outlet capping.

aquifer's submarine outlet is covered by a thin layer of sediment with different permeability (outlet capping, see Figure 1). Assume that the aquifer is horizontal, homogeneous and of uniform thickness, and that the change of water storage in the outlet capping can be neglected. The flow in the confined aquifer is horizontal and follows Darcy's law.

[6] Let the x axis be perpendicular to the coastline, horizontal and positive landward, and the intersection with the coastline be the origin of the axis (see Figure 1). On the basis of the above assumptions the following governing equations can be used to describe the head fluctuation within the confined aquifer [van der Kamp, 1972]:

[7] In the offshore aquifer

$$S_S \frac{\partial h}{\partial t} = K \frac{\partial^2 h}{\partial x^2} + S_S L_e \frac{\partial h_s}{\partial t}, \quad -L < x < 0, \quad -\infty < t < +\infty, \quad (1)$$

In the inland aquifer

$$S_S \frac{\partial h}{\partial t} = K \frac{\partial^2 h}{\partial x^2}, \quad x > 0, \quad -\infty < t < +\infty, \quad (2)$$

where $h(x, t)$, S_S and K are the hydraulic head [L], specific storage [L^{-1}] and hydraulic conductivity [LT^{-1}] of the confined aquifer, respectively; L_e is the loading efficiency (dimensionless) of the sea tide; and $h_s(t)$ is the sea level [L]. Because of the linearity of the model, only one tidal constituent is considered and the sea level is assumed to be

$$h_s(t) = A \cos(\omega t) \quad (3a)$$

where A is the amplitude [L] of the tidal fluctuation, ω is the frequency [T^{-1}] defined as

$$\omega = 2\pi/t_0 \quad (3b)$$

in which t_0 is the tidal period [T]. Here the datum is set to be the mean sea level.

[8] The loading efficiency was defined by van der Kamp and Gale [1983] to describe the formation pressure change caused by an areally distributed change of pressure at land surface. When the compressibility of the solid fraction of the aquifer is negligible, the loading efficiency equals [van der Kamp and Gale, 1983]

$$L_e = \frac{\alpha}{\alpha + n\beta} \quad (4)$$

where α is the vertical compressibility [$M^{-1}LT^2$] of the skeletal aquifer, β is the compressibility [$M^{-1}LT^2$] of pore water in the confined aquifer, and n is the porosity (dimensionless) of the aquifer. The loading efficiency defined by equation (4) was termed "amplitude factor" by Jacob [1950] and Ferris [1951]. Following Jacob [1940], another term, "tidal efficiency," was also used for the quantity given by (4) by many successors such as Carr [1971], Li and Chen [1991a, 1991b], and Li and Jiao [2001a].

[9] It is assumed that there is no inland recharge, so no-flow boundary condition is used at places sufficiently far from the coastline, i.e.,

$$\left. \frac{\partial h}{\partial x} \right|_{x=+\infty} = 0 \quad (5)$$

At the coastline $x = 0$, using the continuity of hydraulic head and flux, respectively, yields

$$\lim_{x \downarrow 0} h(x, t) = \lim_{x \uparrow 0} h(x, t), \quad (6)$$

$$\lim_{x \downarrow 0} \frac{\partial h}{\partial x} = \lim_{x \uparrow 0} \frac{\partial h}{\partial x}. \quad (7)$$

At the aquifer's subcrop $x = -L$, an outlet capping separates the groundwater in the confined aquifer from the seawater. The difference of the hydraulic head between the left and the right sides of the outlet capping is $(h_s - h)$. Neglecting the elastic storage in the outlet capping, the flux between the outlet capping and the aquifer is equal to that between

the sea and the outlet capping, which can be expressed in Darcy's law as

$$-K \left. \frac{\partial h}{\partial x} \right|_{x=-L} = K' \frac{h_s - h}{m} \quad (8a)$$

where K' is the hydraulic conductivity of the outlet capping [LT^{-1}] and m is its thickness [L]. The leaky boundary condition (8a) for the outlet capping can be rewritten as

$$-\left. \frac{\partial h}{\partial x} \right|_{x=-L} + \mu h = \mu h_s \quad (8b)$$

where μ is defined as

$$\mu = \frac{K'}{mK}. \quad (8c)$$

This new parameter μ could be viewed as the relative leakance [L^{-1}] of the outlet capping with respect to the aquifer. It is equal to zero for an impermeable outlet capping and tends to infinity if the outlet capping does not exist (i.e., the width m tends to zero).

2.2. Analytical Solution

[10] The solution of the boundary value problem (1), (2), (5), (6), (7) and (8b) is (see Appendix A for the derivation)

$$h(x, t) = AL_e \left[\cos(\omega t) - \frac{1}{2} e^{ax} \cos(\omega t + ax) + h_0(x, t) \right], \quad -L < x < 0, \quad (9a)$$

$$h(x, t) = AL_e \left[\frac{1}{2} e^{-ax} \cos(\omega t - ax) + h_0(x, t) \right] = ACe^{-ax} \cos(\omega t - ax - \varphi), \quad x > 0, \quad (9b)$$

where

$$h_0(x, t) = \frac{1}{2} \frac{\sqrt{\sigma^4 + 4}}{\sigma^2 + 2\sigma + 2} e^{-(x+2L)a} \cos[\omega t - (x+2L)a - \psi_1] + \frac{\sigma}{\sqrt{\sigma^2 + 2\sigma + 2}} \frac{1 - L_e}{L_e} e^{-(x+L)a} \cdot \cos[\omega t - (x+L)a - \psi_2], \quad (9c)$$

where the parameter a [L^{-1}] is defined as

$$a = \sqrt{\omega S_S / 2K} = \sqrt{\pi S_S / K t_0}, \quad (9d)$$

which can be termed as the confined aquifer's tidal propagation parameter. The parameter σ is the dimensionless leakance defined as

$$\sigma = \frac{\mu}{a} = \frac{K'}{amK}, \quad (9e)$$

and ψ_1 and ψ_2 are the constant phase shifts (in radian) given by

$$\psi_1 = \arctan \frac{2\sigma}{\sigma^2 - 2}, \quad (9f)$$

$$\psi_2 = \arctan \frac{1}{1 + \sigma}, \quad (9g)$$

The coefficient C and phase shift φ in equation (9b) depend on the model parameters a , L , L_e and σ , and are defined as

$$C(aL, L_e, \sigma) = \sqrt{(\eta + L_e/2)^2 + \xi^2}, \quad (9h)$$

$$\varphi(aL, L_e, \sigma) = \arctan \frac{2\xi}{2\eta + L_e}, \quad (9i)$$

where

$$\eta = \frac{L_e e^{-aL}}{\sigma^2 + 2\sigma + 2} \left\{ \frac{e^{-aL}}{2} [(\sigma^2 - 2) \cos(2aL) - 2\sigma \sin(2aL)] + \frac{1 - L_e}{L_e} [(\sigma^2 + \sigma) \cos(aL) - \sigma \sin(aL)] \right\}, \quad (9j)$$

$$\xi = \frac{L_e e^{-aL}}{\sigma^2 + 2\sigma + 2} \left\{ \frac{e^{-aL}}{2} [2\sigma \cos(2aL) + (\sigma^2 - 2) \sin(2aL)] + \frac{1 - L_e}{L_e} [(\sigma^2 + \sigma) \sin(aL) + \sigma \cos(aL)] \right\}. \quad (9k)$$

3. Discussions and Application

3.1. Comparisons With Existing Analytical Solutions

[11] The analytical solution for the groundwater head fluctuation of the confined aquifer offshore is given by equation (9a) and inland by equation (9b). Equations (9a)–(9k) contain four independent parameters: the dimensionless leakance σ , the offshore extending length L , the confined aquifer's tidal propagation parameter a , and the loading efficiency L_e . For the cases that the outlet capping's dimensionless leakance and/or the aquifer's offshore extending length are either zero or infinity, the new analytical solution (9a) and (9b) can be simplified into the existing analytical solutions obtained by the previous researchers.

3.1.1. Aquifer Extending Under the Sea Infinitely

[12] For a confined aquifer that extends under the sea infinitely ($L \rightarrow +\infty$), in view of (9a) and (9b), one obtains

$$h(x, t) = AL_e \left[-\frac{1}{2} e^{ax} \cos(\omega t + ax) + \cos(\omega t) \right], \quad x < 0, \quad (10a)$$

$$h(x, t) = \frac{1}{2} AL_e e^{-ax} \cos(\omega t - ax), \quad x \geq 0, \quad (10b)$$

which is essentially the same as the result derived by *van der Kamp* [1972]. In this case, all the parameters relating to the outlet capping disappear. In fact, in the model, when the offshore extending length approaches infinity, the outlet capping vanishes automatically and the head fluctuation in the aquifer is completely decided by the loading efficiency L_e and the aquifer's tidal propagation parameter a .

3.1.2. Aquifer With Zero Offshore Extending Length

[13] For a confined aquifer which terminates at the coastal line, the offshore extending length $L = 0$, then by means of (9b) it follows that

$$h(x, t) = Ae^{-ax} \frac{\sigma}{\sqrt{\sigma^2 + 2\sigma + 2}} \cdot \cos\left(\omega t - ax - \arctan \frac{1}{1 + \sigma}\right), \quad x \geq 0, \quad (11)$$

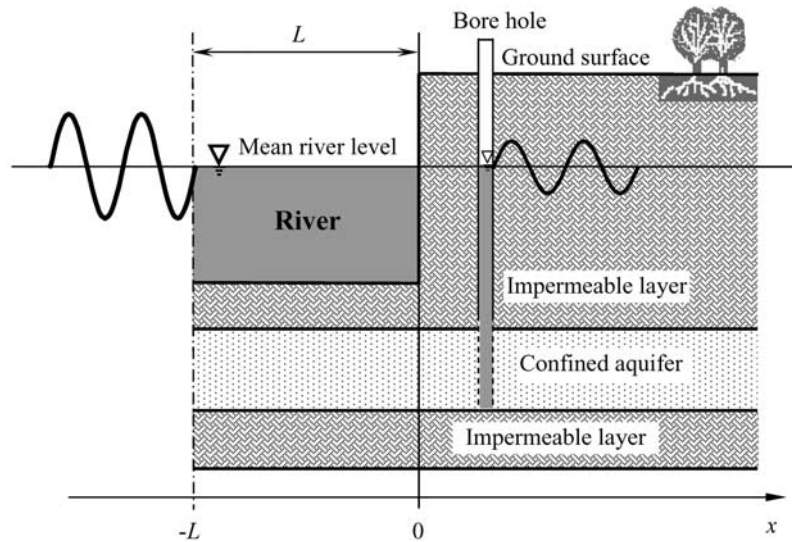


Figure 2. Schematic of a confined aquifer extending under a tidal river.

where the dimensionless leakage σ is defined as (9e). The loading efficiency L_e disappears automatically in equation (11), in agreement with reality. The tidal loading effect acts through the offshore extending roof by causing elastic compression and expansion of both the aquifer skeleton and the pore water. When $L = 0$, there is no aquifer under the sea, subsequently the loading effect of the tidal water above the aquifer and the loading efficiency L_e vanish. Compared with the widely used *Jacob* [1950] solution, the existence of the outlet capping diminishes the amplitude of the groundwater head fluctuation by the ratio

$$r_c = \frac{\sigma}{\sqrt{\sigma^2 + 2\sigma + 2}} \quad (12a)$$

and leads also to an extra phase shift corresponding to a spatially constant time lag equal to

$$\Delta t_{c-lag} = \frac{1}{\omega} \tan^{-1} \frac{1}{1 + \sigma} = \frac{1}{\omega} \tan^{-1} \frac{amK}{amK + K'} \quad (12b)$$

[14] When the dimensionless leakage σ changes from 0 (impermeable outlet capping) to infinity (without outlet capping), the amplitude coefficient r_c increases from 0 to 1 (curve corresponding to $aL = 0$ shown in Figure 7a), while the time lag Δt_{c-lag} decreases from $\pi/(4\omega)$ to zero (curve corresponding to $aL = 0$ shown in Figure 7b). As the dimensionless leakage $\sigma \rightarrow +\infty$, which means that the outlet capping's thickness $m \rightarrow 0$, the amplitude coefficient $r_c \rightarrow 1$ and the time lag $\Delta t_{c-lag} \rightarrow 0$. In this case the solution simply becomes the *Jacob* [1950] solution. When the dimensionless leakage $\sigma \rightarrow 0$, the amplitude coefficient $r_c \rightarrow 0$, in this case the groundwater head in aquifer will not respond to the tidal fluctuation in the sea.

3.1.3. Aquifer With an Impermeable Outlet Capping

[15] For an aquifer with impermeable outlet capping, let $\sigma \rightarrow 0$ in equations (9a), (9b), (9c), (9j) and (9k), one has

$$h(x, t) = AL_e \left[\cos \omega t - \frac{e^{ax}}{2} \cos(\omega t + ax) + e^{-a(x+2L)} \cdot \cos(\omega t - a(x+2L)) \right], \quad -L < x < 0, \quad (13a)$$

$$h(x, t) = x \frac{L_e e^{-ax}}{2} A \sqrt{1 - 2e^{-2aL} \cos(2aL) + e^{-4aL}} \cdot \cos \left[\omega t - ax + \arctan \frac{e^{-2aL} \sin(2aL)}{1 - e^{-2aL} \cos(2aL)} \right], \quad x > 0. \quad (13b)$$

In this case, the groundwater head fluctuation depends on the loading efficiency L_e and the dimensionless extending length aL . At the coastline $x = 0$, if $2aL < \pi$, equation (13b) indicates a negative phase shift leading to a “time advance” equal to

$$\Delta t_{advance} = \frac{1}{\omega} \arctan \frac{e^{-2aL} \sin(2aL)}{1 - e^{-2aL} \cos(2aL)}. \quad (13c)$$

Equations (13a), (13b) and (13c) can be used not only to describe the tidal fluctuation in a confined coastal aquifer with an impermeable outlet capping, but also to describe the head responses of a confined aquifer under a tidal river to its water level fluctuation. Assume that the river is straight, symmetric with respect to its middle line and has a width of $2L$, the aquifer is horizontal and separated by an impermeable layer from the river. The tidal flow in the aquifer is one-dimensional and perpendicular to the river bank (see Figure 2). Because the symmetric boundary condition at the river middle line is equivalent to the boundary condition of the impermeable outlet capping here, equations (13a), (13b), and (13c) give the head fluctuation in the aquifer under the river with $x = 0$ at the river bank and $x = -L$ at the river middle line.

[16] When $aL \rightarrow 0$, the time advance reaches its maximum $\pi/(4\omega)$. This means that for very small offshore roof length, there may exist a time advance of about 3 hours for diurnal tide and 1.5 hours for semidiurnal tide. This has been observed in the field. For example, the groundwater heads in several piezometers near the shallow tidal river Hollandsche IJssel at Gouderak, the Netherlands, were running ahead of the river tide by more than an hour [*Maas and De Lange*, 1987]. Particularly, the observed data from a piezometer at the river bank has an amplitude attenuation of 0.115 and a time advance of 65–85 min. *Maas and De Lange* [1987] called this observed negative phase shift of

tidal groundwater flow “The Gouderak anomaly” and conducted an analytical study based on a tidal fluctuation model of an aquitard-aquifer system under a tidal river. Using the following data: $\omega = 12.3 \text{ d}^{-1}$, $S = 5 \times 10^{-4}$, $T = 850 \text{ m}^2\text{d}^{-1}$, $L = 45 \text{ m}$, $L_e = 1$, $c = 2000 \text{ d}$ (the ratio of the thickness to the vertical permeability of the aquitard between the river and the aquifer), which are believed to cover the Gouderak situation, *Maas and De Lange* [1987] estimated a time advance of 79.2 min and an amplitude ratio of 0.11, which are in line with the observations.

[17] If the leakage of the aquitard is negligible (i.e., let the thickness-permeability ratio $c \rightarrow \infty$) and assume $L_e = 1$, the model of *Maas and De Lange* [1987] is the same as the situation considered here. Consequently, the amplitude and time shift at the river bank given by (9a) in their paper are essentially the same as those given by equation (13b) at $x = 0$. In this case, equation (13b) gives a time advance of 82.2 min and an amplitude ratio of 0.111 at $x = 0$, which are also in line with the observations. This implies that the aquitard’s leakage is negligible. More examples of observed time advance in aquifers under tidal river are given by *Maas and De Lange* [1987].

3.1.4. Aquifer Without Outlet Capping

[18] For aquifers without outlet capping, i.e., the thickness of outlet capping $m = 0$, which is equivalent to $\sigma = \infty$ in view of (9e). Let $\sigma \rightarrow \infty$ in (9j) and (9k), η and ξ can be simplified as

$$\lim_{\sigma \rightarrow \infty} \eta = e^{-aL} \left[\frac{e^{-aL}}{2} L_e \cos(2aL) + (1 - L_e) \cos(aL) \right], \quad (14a)$$

$$\lim_{\sigma \rightarrow \infty} \xi = e^{-aL} \left[\frac{e^{-aL}}{2} L_e \sin(2aL) + (1 - L_e) \sin(aL) \right]. \quad (14b)$$

The solution given by (9b), (9h), (9i) and (14) is essentially the same as the solution given by equations (16a), (16b) and (16c) of *Li and Jiao* [2001a] when the leakage through the semiconfining layer is negligible.

3.2. Case Study in a Coastal Aquifer in the Jahe River Basin, Shandong, China

[19] The study area is located in the west part of the estuary of the Jahe River in Yantai City, Shandong Province, China. The northern boundary of the area is the several kilometers long and relatively straight coastline of the Yellow sea (Figure 3). This coastal aquifer system consists of five layers, as shown illustratively in Figure 4. The lowest layer, which is approximately 18 m thick and has an impermeable bedrock bottom about 46 m deep from the ground surface, is the main aquifer for groundwater extraction in this area. The top layer terminates at the coastline and each of the 4 lower layers extends under the sea for a certain length. The case study here will focus on the main aquifer only. Several large groundwater drawdown cones were formed due to long-term groundwater exploitation in the main aquifer. The observation well GK2A, which is screened in the main aquifer, is about 200 m landward from the coastline and 2000 m from the west bank of Jahe River.

[20] Compared with the very permeable alluvial gravel with pebbles of the main aquifer, the sandy clay and silt layer immediately above it can be treated as impermeable

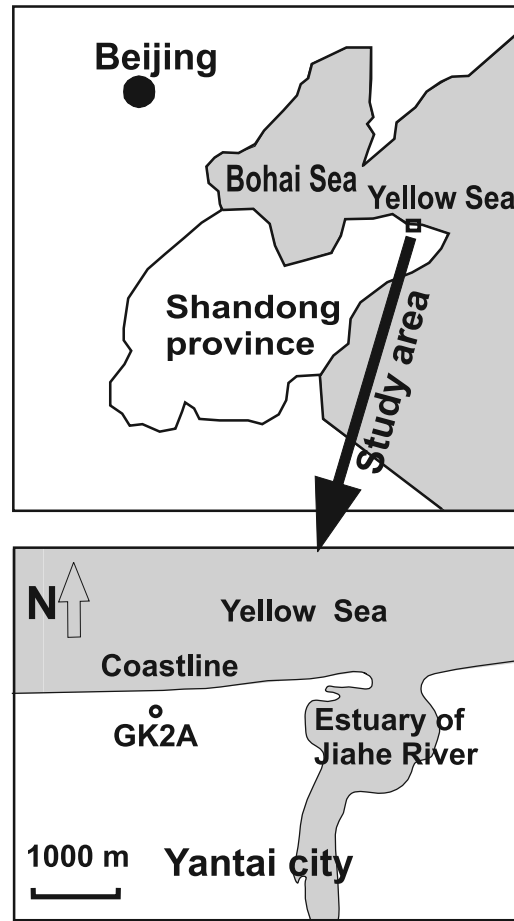


Figure 3. Location map of the observation well GK2A [after *Cheng et al.*, 2004].

(or confining). In addition, the impact of the tidal boundary of the Jahe River on the head fluctuation at GK2A can be neglected because the river bank is much far from the well than the coastline is. Therefore the solution (9b) can be used to describe the head fluctuation in the observation well GK2A assuming one dimensional groundwater flow in the southern direction (see Figure 3). The observed tidal level in the sea and groundwater head fluctuation in the well GK2A during 3 and 4 August 1998 are reported in Figure 5. One can see that the head fluctuation at GK2A is synchronous with the sea tide (i.e., no time lag). This phenomenon cannot be explained using the traditional solutions such as *Jacob* [1950], *Li and Jiao* [2001a], and *Li and Jiao* [2002a] that always predict a significant time lag between the tide and the head at GK2A. However, by hypothesizing the presence of a silt skin zone at the submarine outlet, the synchronous fluctuations can be explained based on the solution given by equation (9b).

[21] The tidal fluctuation can be approximated by the superposition of the semidiurnal ($\omega_1 = 0.253 \text{ h}^{-1}$) and diurnal ($\omega_2 = 0.506 \text{ h}^{-1}$) components:

$$H_{\text{Sea}}(t) = W_{\text{Sea}} + A_{\text{Sea},1} \cos(\omega_1 t - \theta_{\text{Sea},1}) + A_{\text{Sea},2} \cos(\omega_2 t - \theta_{\text{Sea},2}), \quad (15)$$

where W , A , ω and θ are the mean elevation [L], amplitude [L], frequency [T^{-1}], and the phase shift [radian] of the tidal fluctuation, respectively; the subscripts $j = 1, 2$ represent the

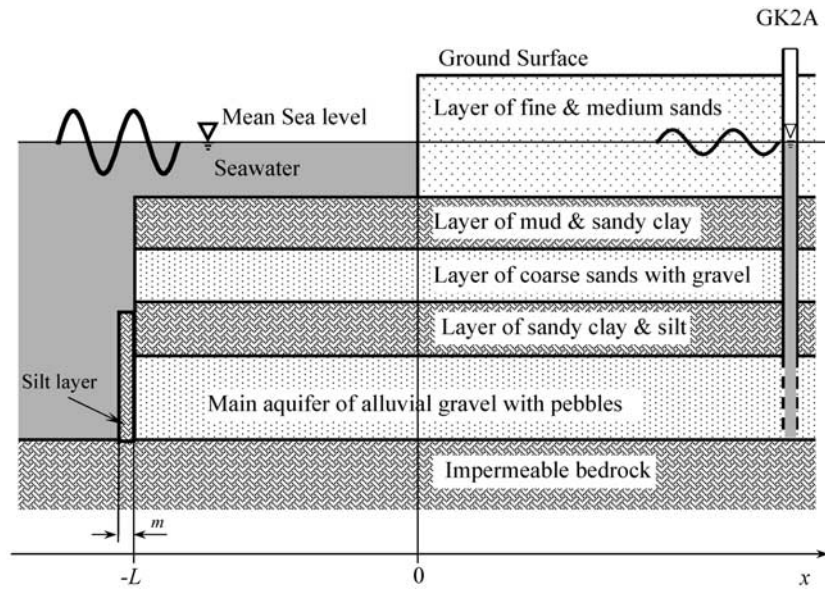


Figure 4. Schematic of the vertical cross section through GK2A vertical to the coastline [after Cheng *et al.*, 2004].

semidiurnal and diurnal components, respectively. The fit of equation (15) to the observed tidal variation was good (Figure 5), and gave the parameter values reported in Table 1. Of interest is the mean elevation, W , which was found to be 0.344 m.

[22] On the basis of the superposition principle, assume that the diurnal and semidiurnal components of the head fluctuation at GK2A are respectively caused by the diurnal and semidiurnal components of the tide. The solution (9b) can be used to describe the tide-induced head fluctuation at GK2A as follows:

$$h_{GK2A}(x_0, t; W_{GK2A}, L_e, a_1x_0, a_1L, \sigma_1) = W_{GK2A} + \sum_{j=1}^2 A_{Sea,j} C_j e^{-a_j x_0} \cos(\omega_j t - a_j x_0 - \phi_j - \theta_{Sea,j}), \quad (16)$$

where $x_0 = 200$ m, the subscript $j=1$ of all the parameters represents the semidiurnal component, and $j=2$ for diurnal component; W_{GK2A} is the mean head at GK2A. There are five independent parameters in equation (16): W_{GK2A} , L_e , a_1x_0 , a_1L and σ_1 (because $a_1 = a_2\sqrt{\omega_1/\omega_2}$ and $\sigma_1 = \sigma_2\sqrt{\omega_2/\omega_1}$). Knowledge of their values ensures knowledge of the head fluctuation at well GK2A.

3.3. Parameter Estimation

[23] A least squares type objective function is adopted for estimate of the 5 parameters:

$$F = \sum_{j=1}^{37} [h_{GK2A}(x_0, t_j; W_{GK2A}, L_e, a_1x_0, a_1L, \sigma_1) - h_j^*]^2 + \left[L_e - \frac{2K(a_1x_0)^2 - n\rho_w g \beta \omega_1 x_0^2}{2K(a_1x_0)^2} \right]^2 \quad (17)$$

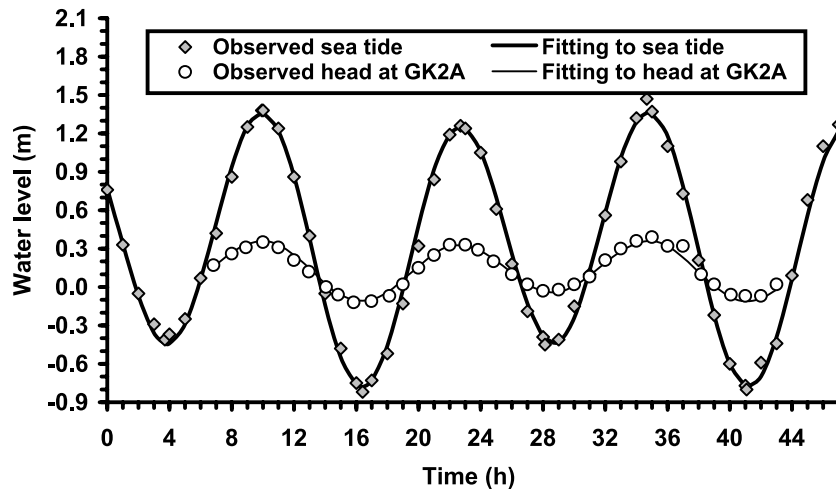


Figure 5. Observed sea level and hydraulic head data at GK2A during 3 and 4 August 1998 and their least squares fittings. The beginning time is 0000 on 3 August 1998, a constant 0.134 m is added to the least squares fittings based on equation (16), and the curves of the three different least squares fittings to the head at GK2A listed in Table 1 coincide with each other.

Table 1. Fitting Results of Observed Tidal Level and Head at GK2A

	W , m	A_1 , m	θ_1 , rad	A_2 , m	θ_2 , rad	RLS, ^a m ²
Least squares fitting of tidal level in the sea	0.34	0.181	1.325	0.95	5.116	0.1925
Direct least squares head fitting at GK2A	0.13	0.0425	1.490	0.207	5.093	0.0225
Head fitting at GK2A by minimizing (20) when $n = 0.1$	0.13	0.0385	1.478	0.208	5.095	0.0228
Head fitting at GK2A by minimizing (20) when $n = 0.2$	0.13	0.0373	1.433	0.209	5.098	0.0231

^aResidual of least squares, namely, the sum of the squares of the differences between the observed data and theoretical prediction.

The first bracket represents the sum of the squared residuals, which is standard approach in least squares estimation. The second term represents a constraint as a penalty function. This term alleviates the problem of nonuniqueness common to estimation of aquifer parameters as explained by *Carrera and Neuman* [1986; see also *Boufadel et al.*, 1998].

[24] The development of the penalty term is based on the following considerations. The site investigation near GK2A indicated a rough aquifer permeability estimation of $K = 30$ m/d [*Cheng*, 1999]. In addition, the porosity n has a much more narrow value range than the other aquifer parameters and it is not unreasonable to assume $n = 0.1-0.2$. To incorporate the above information in the parameter estimations properly, an intrinsic relation among the parameters K , n , L_e and a_1x_0 is found and used. Using the equation $S_S = \rho_w g(\alpha + n\beta)$ [*Fetter*, 1994], where $\rho_w = 1000$ kg/m³ is the water density, $\beta = 4.6 \times 10^{-10}$ m²/N is the water compressibility and $g = 9.8$ m/s² is the gravity acceleration, equation (4) can be rewritten as

$$L_e = \frac{\alpha}{\alpha + n\beta} = \frac{\rho_w g \alpha}{S_S} = \frac{S_S - n\rho_w g \beta}{S_S}, \quad (18)$$

Using (9d), one has $S_S = 2Ka_1^2/\omega_1$. Substituting this into equation (18), yields

$$L_e - \frac{2K(a_1x_0)^2 - n\rho_w g \beta \omega_1 x_0^2}{2K(a_1x_0)^2} = 0. \quad (19)$$

With the rough information of K and n , equation (19) provides an approximate intrinsic relationship among the parameters, on which the penalty term in equation (17) is based.

[25] A Fortran code was developed to minimize the objective function defined by equation (17) using the quasi-Newton iteration method. The minimization was with respect to the quantities W_{GK2A} , L_e , $\log(a_1x_0)$, $\log(a_1L)$ and $\log\sigma_1$. The logarithm was used on parameters whose range was large (the range of L_e is from 0 to 1), because such an approach can speed convergence to the solution and avoid the computation of negative parameter values in the iteration [e.g., *Carrera and Neuman*, 1986; *Li and Yang*, 2000; *Li et al.*, 2004]. Various initial guesses were considered, and the global optimum was found at the parameters' values reported in the third row of Table 1. The global minimum was 0.0228 m², which is only slightly greater than the residual obtained from the direct least squares value (0.0225 m²) assuming that the response of GK2A consists of two components (similar to what was assumed for the tidal fluctuations described by equation (15); see Table 1). This indicates that the constraint (equation (19)) implemented by the penalty term did not greatly alter the location

of the optimum, rather “nudged” the search algorithm a little. For all the different initial parameter guess values, the converged parameter values of W_{GK2A} , L_e , a_1x_0 , a_1L and σ_1 are the same if the global minimum is reached. The values of these parameters is listed in Tables 1 (W_{GK2A}) and 2 (the other four parameters). The difference between $W_{GK2A} = 0.13$ m and $W_{Sea} = 0.34$ m may be due to the foregoing groundwater drawdown cones and the tidal wave setup near the coastline.

[26] Using the value of a_1x_0 and $x_0 = 200$ m, the aquifer's wave number a_1 can be estimated, then the extending length L of the aquifer can be obtained from the value of a_1L , and finally the permeability K' of the silt outlet capping can be estimated. In fact, from equation (9e), the leakage of the silt outlet capping is $K'/m = \sigma_1 a_1 K \approx 4.83 \times 10^{-3}$ d⁻¹. Assuming that the thickness m of the silt outlet capping is on the order of 1 m, then the order of magnitude of K' ranges from 10⁻³ m/d to 10⁻² m/d. This estimation is within the permeability value ranges for silt, sandy silt and silty sands in Table 3.7 of *Fetter* [1994].

[27] To examine the impact of the porosity on the parameter estimation results, the objective function (20) was minimized for $n = 0.2$. The results are listed in the last rows of Tables 1 and 2, where one can see that the discrepancies between the estimated parameters for $n = 0.1$ and 0.2 are very small, confirming our initial hypothesis that the porosity does not greatly affect the head values. This was also noted by *Boufadel et al.* [1998] and *Boufadel* [2000].

[28] The estimated leakage of the silt outlet capping is very small, indicating a very weak hydraulic connection between the seawater and the aquifer pore water at the submarine outlet of the main aquifer. The significant head fluctuation at GK2A is mainly caused by the tidal loading onto the several hundred meters long aquifer roof. The synchronous fluctuation of the hydraulic head at GK2A with the sea level is caused by the less permeable silt sediment at the aquifer's submarine outlet.

4. Analyses of Inland Aquifer Responses

4.1. Approximation for Small Offshore Roof Length

[29] If the dimensionless extending length aL is small enough for its terms of high order greater than or equal to 2 to be neglected, that is, if

Table 2. Estimated Aquifer Parameters Near GK2A When the Porosity n Assumes 0.1 and 0.2

n	L_e	$a_1 x_0$	$a_1 L$	σ_1	a_1 , m ⁻¹	L , m	K'/m , d ⁻¹
0.1	0.78	0.092	0.21	0.35	0.00046	460	0.0048
0.2	0.76	0.12	0.25	0.31	0.00060	420	0.0056

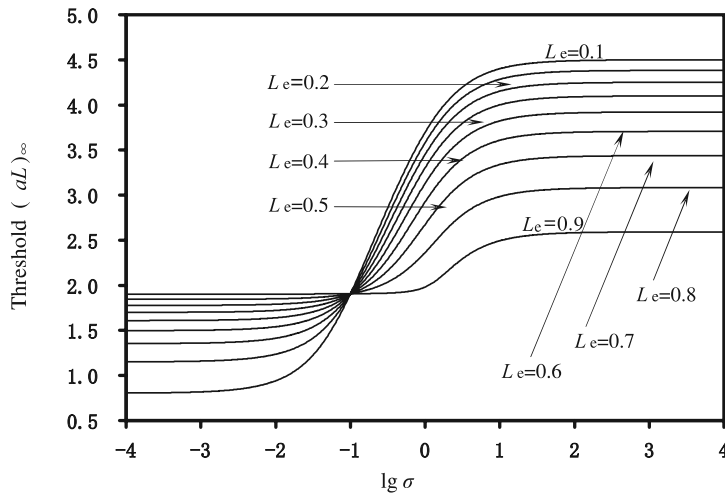


Figure 6. Change of the threshold $(aL)_\infty$ with the dimensionless leakage of the outlet capping for different values of loading efficiency L_e .

$$\begin{aligned} \exp[-aL(1+i)] &= 1 - aL(1+i) + O(a^2L^2), \\ \exp[-2aL(1+i)] &= 1 - 2aL(1+i) + O(a^2L^2), \end{aligned} \quad (20a)$$

then the complex coefficient $C_4 = \frac{L_e}{2} + \eta - i\xi$ in Appendix A can be simplified as follows:

$$\begin{aligned} C_4 &= \frac{L_e}{2} + \eta - i\xi \\ &= L_e \left\{ \frac{1}{2} + \frac{\sigma - 1 - i}{2(\sigma + 1 + i)} \exp[-2a(1+i)L] \right. \\ &\quad \left. - \frac{\sigma}{\sigma + 1 + i} \exp[-a(1+i)L] \right\} + \frac{\sigma}{\sigma + 1 + i} \exp[-a(1+i)L] \\ &= L_e \frac{2iaL}{\sigma + 1 + i} + \frac{\sigma}{\sigma + 1 + i} \exp[-a(1+i)L] + O(a^2L^2) \\ &= \frac{\sigma}{\sigma + 1 + i} \exp[-a(1+i)L] + O\left(\frac{2L_e aL}{\sqrt{\sigma^2 + 2\sigma + 2}}\right) \end{aligned} \quad (20b)$$

If $\sigma \geq O(1)$, substituting the values of η and ξ determined by (20b) back into (9b) yields

$$\begin{aligned} h(x,t) &\approx Ae^{-a(x+L)} \frac{\sigma}{\sqrt{\sigma^2 + 2\sigma + 2}} \\ &\quad \cdot \cos[\omega t - a(x+L) - \varphi_2], \quad x > 0, \quad \sigma \geq O(1). \end{aligned} \quad (21)$$

Compared (21) with (11) where the offshore extending length is zero, it is found that when aL is small enough, the groundwater fluctuation in the inland aquifer behaves as if the coastline were extended seaward to the aquifer's submarine outlet where $x = -L$. Using equations (20b), (A1), (A2), (A9b), (A12) and (A13), one can find that the error of the approximation (21) has an order of $O\left(\frac{\sqrt{2L_e aL}}{\sqrt{\sigma^2 + 2\sigma + 2}}\right)$. Let ε be the tolerance of the approximation error, a threshold value of aL can be determined by $\frac{\sqrt{2L_e aL}}{\sqrt{\sigma^2 + 2\sigma + 2}} \leq \varepsilon$, namely,

$$(aL)_0 = \frac{\varepsilon \sqrt{\sigma^2 + 2\sigma + 2}}{\sqrt{2L_e}}, \quad (22)$$

so that if $L \leq L_0$, the aquifer's submarine outlet can be regarded as the coastline. As can be seen from (21), when $L \leq L_0$, the head fluctuations are independent of the loading efficiency L_e , and the independent parameters of the system is reduced to three only, i.e., a , L and σ . The above discussion indicates that for the case that the aquifer's offshore length is small enough and the outlet capping is relatively permeable ($\sigma \geq O(1)$), the loading effect of the sea tide above the aquifer can be neglected.

4.2. Approximation for Great Offshore Roof Length

[30] For the case that the offshore aquifer length is infinity ($L = \infty$), the responses in inland aquifer is given by equation (10b). Here it will be shown that if the dimensionless extending length aL is great enough, the inland tidal fluctuation can be approximated by equation (10b). Because the coefficient C and phase shift φ in equation (9b) are the magnitude and argument of the coefficient C_4 in Appendix A. The error between (9b) and (10b) relative to the local tidal amplitude Ae^{-ax} can be estimated as follows.

$$\begin{aligned} &\left| C \cos(\omega t - ax - \varphi) - \frac{L_e}{2} \cos(\omega t - ax) \right| \\ &= \left| \operatorname{Re} \left\{ C_4 \exp[-i(ax + \omega t)] - \frac{L_e}{2} \exp[-i(ax + \omega t)] \right\} \right| \\ &\leq \left| C_4 \exp[-i(ax + \omega t)] - \frac{L_e}{2} \exp[-i(ax + \omega t)] \right| = \left| C_4 - \frac{L_e}{2} \right| \\ &= |\eta - i\xi| = \left| \frac{\sigma - 1 - i}{\sigma + 1 + i} \cdot \frac{L_e}{2} \exp[-2a(1+i)L] \right. \\ &\quad \left. + \frac{\sigma(1-L_e)}{\sigma + 1 + i} \exp[-a(1+i)L] \right| \\ &\leq \exp(-2aL) \left| \frac{\sigma - 1 - i}{\sigma + 1 + i} \cdot \frac{L_e}{2} \right| + \exp(-aL) \left| \frac{\sigma(1-L_e)}{\sigma + 1 + i} \right|, \end{aligned} \quad (23)$$

therefore, for a finite extending length which satisfies $\exp(-aL) \ll 1$, equation (10b) can approximately describe the inland tidal fluctuation with an absolute error less than

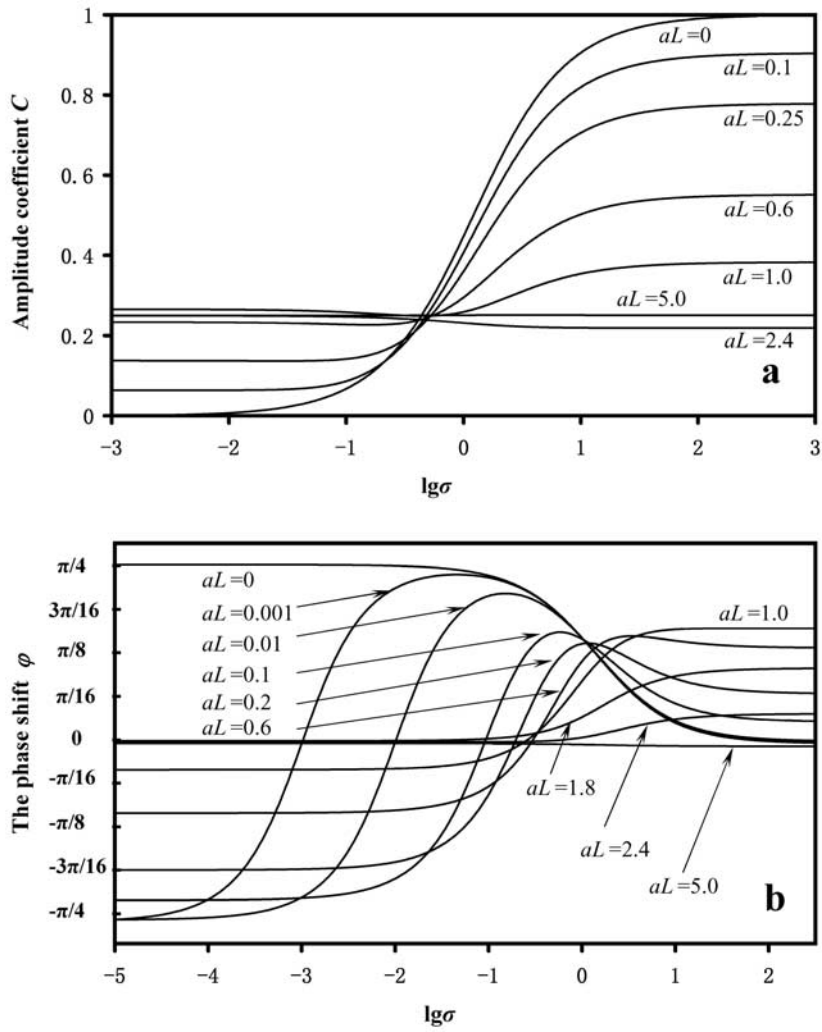


Figure 7. Changes of (a) the amplitude coefficient C and (b) the phase shift φ with dimensionless leakage for different values of dimensionless extending length aL when loading efficiency $L_e = 0.5$.

$$\varepsilon = \exp(-2aL) \left| \frac{\sigma - 1 - i}{\sigma + 1 + i} \cdot \frac{L_e}{2} \right| + \exp(-aL) \left| \frac{\sigma(1 - L_e)}{\sigma + 1 + i} \right|. \quad (24)$$

Let ε be the tolerance of the approximation error (the detection limit of the water level measurement device), solving equation (24) for aL , one obtains the threshold value of the dimensionless extending length

$$(aL)_\infty = \ln \left[L_e \sqrt{\sigma^2 - 2\sigma + 2} \right] - \ln \left[\sqrt{\sigma^2(1 - L_e)^2 + 2\varepsilon L_e \sqrt{\sigma^4 + 4} - \sigma(1 - L_e)} \right]. \quad (25)$$

Equation (25) is helpful to analyze the influence of the offshore roof length on the inland groundwater fluctuation. For a real aquifer system, if its dimensionless extending length satisfies $aL \geq (aL)_\infty$, then the inland aquifer response given by (9b) is approximately the same as that by (10b). In this case, the tidal propagation in the inland aquifer will behave as if the offshore roof length were infinite. Figure 6 shows how the threshold $(aL)_\infty$ changes with the outlet capping's dimensionless leakage for different values of loading efficiency L_e . The threshold

increases strictly with the dimensionless leakage for fixed loading efficiency.

4.3. Tidal Fluctuation in the Inland Aquifer

[31] The tidal fluctuation in the inland aquifer is characterized by equation (9b). Comparison of (9b) with the simple *Jacob* [1950] solution indicates that the existences of the offshore aquifer and the outlet capping reduce the amplitude by a coefficient C and change the phase by a shift φ , with C and φ depending on the parameters σ , aL and L_e . Given C and φ , the aquifer head fluctuation at the coastline is described by $AC \cos(\omega t - \varphi)$. Regarding the coastline as the boundary of the inland aquifer, and using the *Jacob* [1950] solution, one can easily conclude that the head in the inland aquifer is $ACe^{-ax} \cos(\omega t - ax - \varphi)$. This is a simple explanation to the solution (9b) from the viewpoint of *Jacob's* [1950] solution.

[32] Figure 7a shows how the amplitude coefficient C changes with the outlet capping's dimensionless leakage σ for different values of the dimensionless extending length aL when the loading efficiency $L_e = 0.5$. The following observations can be made from Figure 7a. When aL is

small, the amplitude coefficient C increases with the dimensionless leakance σ strictly, as is shown by curves for $aL < 0.45$ in Figure 7a. When $aL \geq 0.45$, the amplitude coefficient C does not always increase with σ . With the increase of aL , the amplitude coefficient C gradually becomes insensitive to changes of σ and converges to the constant $L_e/2 = 0.25$. The head fluctuation amplitude at the coastline equals AC , which is influenced by two factors: the tidal loading on the roof and the hydraulic connection with the tidal water through the aquifer's outlet capping. When the aquifer's submarine outlet is close to the coastline, the tidal loading effect is relatively weak because the length of the roof, through which the tidal loading acts, is short. In this case the head fluctuation at the coastline is dominated by the leakance of the outlet capping and increases with σ .

[33] When the offshore roof length is equal to or greater than the threshold L_∞ determined by equation (25), the effect of the outlet capping on the head fluctuation at the coastline becomes negligible. In this case the head fluctuation at the coastline is dominated by the tidal loading through the aquifer's offshore roof, and the coefficient C is close to $L_e/2$, as is suggested by equation (10b) which describes the situation of $L = \infty$.

[34] When the offshore roof length is long enough but less than the threshold L_∞ determined by equation (25), neither the tidal loading nor the leakance of the outlet capping dominates the head fluctuations at the coastline. The joint actions of the tidal loading and outlet capping lead to the complex, nonmonotonic behavior of the amplitude-leakance relationship.

[35] Figure 7b shows how the phase shift φ changes with σ for different values of aL when $L_e = 0.5$. The dependences of φ on σ and aL are complex, nonmonotonous. The following observations can be made from Figure 7b. For an aquifer terminating abruptly at the coastline, i.e., $aL = 0$, the phase shift is always positive (corresponding to a time lag) and decreases with σ monotonously from $\pi/4$ to 0 (also see discussion for equation (11)). For an aquifer with small offshore extending length, a significant negative phase shift approaching $-\pi/4$ (corresponding to a time advance) occurs if the outlet capping is less permeable or impermeable, as detailed by the discussion for equation (13b). If the aquifer's outlet capping is relatively permeable ($\sigma \geq O(1)$), no significant negative phase shift occurs, no matter what the value of aL is. Significant positive phase shift always occurs when $\sigma \geq 1$ and the offshore extending length is long enough but less than the threshold. Figures 7a and 7b can be served as the type curves of the solution (9b) when $L_e = 0.5$.

[36] When the loading efficiency is fixed to be other value within 0 and 1, the changes of C and φ with σ for different values of aL have similar trends as shown in Figures 7a and 7b. Because of space limitation they will not be detailed here.

5. Conclusions

[37] A confined coastal aquifer usually extends offshore for some distance with its submarine outlet covered by a thin layer of sediment (outlet capping) different from the aquifer. Previous theoretical studies neglected the effect of this outlet capping. This paper gives an analytical solution for a confined aquifer subject to tidal fluctuations with a

leaky boundary condition at the aquifer's submarine outlet capping. For the cases that offshore length of the aquifer and/or the leakance of the outlet capping are either zero or infinity, existing solutions in literature are obtained. Particularly, if the offshore aquifer's length is small and the leakance of the outlet capping equals zero, the solution can be used to describe the tidal wave propagation in a confined aquifer under a tidal river separated by an impermeable layer and extending infinitely. The full solution agreed well with the observations in a piezometer in the Jahe River Basin in China, 200 m inland from the coastline where the tide-induced head fluctuations without delay were observed but cannot be explained by previous analytical and numerical solutions which ignore the outlet capping's effect.

[38] The existences of the confined offshore aquifer and its outlet capping reduce the amplitude by a spatially constant coefficient and change the phase by a spatially constant shift, both of which are controlled by the outlet capping leakance and the tidal loading effect. The joint actions of the tidal loading and outlet capping lead to complex dependences of the head fluctuation on the outlet capping's leakance. When the offshore confined aquifer is short, the inland head fluctuation increases with the outlet capping's leakance. In this case significant negative phase shift occurs if the leakance is small. For offshore aquifer length greater than a threshold value, the inland head fluctuations are independent of this length and the outlet capping's leakance.

Appendix A: Derivation of the solution to (1)–(8)

[39] Let $H(x,t)$ be a complex function of the real variables x and t that satisfies the equations (1), (2), (5), (6), (7), and (8b) after the term $h_S(t) = A \cos(\omega t)$ in equations (1) and (8b) is replaced by $A \exp(i\omega t)$, where $i = \sqrt{-1}$. Because $h(x,t)$ is the solution to (1), (2), (5), (6), (7), and (8b), it follows that

$$h(x,t) = \text{Re}(H(x,t)), \quad (\text{A1})$$

where Re denotes the real part of the followed complex expression.

[40] Now suppose

$$H(x,t) = AX(x) \exp(i\omega t), \quad (\text{A2})$$

where $X(x)$ is an unknown function of x . Substituting (A2) into the six equations which $H(x,t)$ satisfies and then dividing the results by $A \exp(i\omega t)$ yield

$$X''(x) - \frac{i\omega S_S}{K} X(x) = -\frac{i\omega S_S}{K} L_e, \quad -L < x < 0, \quad -\infty < t < +\infty, \quad (\text{A3})$$

$$X''(x) - \frac{i\omega S_S}{K} X(x) = 0, \quad x > 0, \quad -\infty < t < +\infty, \quad (\text{A4})$$

$$X'(+\infty) = 0 \quad (\text{A5})$$

$$\lim_{x \downarrow 0} X(x) = \lim_{x \uparrow 0} X(x) \quad (\text{A6})$$

$$\lim_{x \downarrow 0} X'(x) = \lim_{x \uparrow 0} X'(x) \quad (\text{A7})$$

$$X'(-L) - a\sigma X(-L) + a\sigma = 0 \quad (\text{A8})$$

where a is the constant defined by (9d) and σ that by (9e). The general solutions to the equation (A3) and (A4) are

$$X(x) = C_1 \exp[a(1+i)x] + C_2 \exp[-a(1+i)x] + L_e, \quad -L < x < 0, \quad (\text{A9a})$$

$$X(x) = C_3 \exp[a(1+i)x] + C_4 \exp[-a(1+i)x], \quad x > 0, \quad (\text{A9b})$$

where C_1 , C_2 , C_3 and C_4 are four unknown complex constants. By means of equations (A5)–(A8), after some routine calculation, one obtains

$$C_1 = -\frac{L_e}{2}, \quad (\text{A10})$$

$$C_2 = \frac{\sigma - 1 - i}{\sigma + 1 + i} \cdot \frac{L_e}{2} \exp[-2a(1+i)L] + \frac{\sigma(1-L_e)}{\sigma + 1 + i} \exp[-a(1+i)L] \stackrel{\text{def.}}{=} \eta - i\xi, \quad (\text{A11})$$

$$C_3 = 0, \quad (\text{A12})$$

$$C_4 = \frac{L_e}{2} + \frac{\sigma - 1 - i}{\sigma + 1 + i} \cdot \frac{L_e}{2} \exp[-2a(1+i)L] + \frac{\sigma(1-L_e)}{\sigma + 1 + i} \exp[-a(1+i)L] = \frac{L_e}{2} + \eta - i\xi, \quad (\text{A13})$$

where η is the real part of C_2 given by (9j), and ξ , the negative imaginary part of C_2 given by (9k). Substituting (A10)–(A13) into equation (A9a) and (A9b), then into equation (A2), one obtains the complex function $H(x,t)$. Then by means of equation (A1), calculating the real part $h(x,t)$ of the complex function $H(x,t)$, one can obtain the solution $h(x,t)$ given by (9a) and (9b).

[41] **Acknowledgments.** This research was supported by the National Natural Science Foundation of China (40672167). The authors are very grateful to Tammo S. Steenhuis (Associate Editor) for his comments, which improved the paper significantly.

References

- Boufadel, M. C. (2000), A mechanistic study of nonlinear solute transport in a groundwater-surface water system under steady state and transient hydraulic conditions, *Water Resour. Res.*, *36*, 2549–2565.
- Boufadel, M. C., M. T. Suidan, C. H. Rauch, A. D. Venosa, and P. Biswas (1998), 2-D variably-saturated flow: Physical scaling and Bayesian estimation, *J. Hydrol. Eng.*, *3*, 223–231.
- Carr, P. A. (1971), Use of harmonic analysis to study tidal fluctuations in aquifers near the sea, *Water Resour. Res.*, *7*, 632–643.
- Carrera, J., and S. P. Neuman (1986), Estimation of aquifer parameters under transient and steady state conditions: 1. Maximum likelihood method incorporating prior information, *Water Resour. Res.*, *22*, 199–210.
- Cheng, J. M. (1999), Three-dimensional seawater intrusion in multilayered aquifer system: Formulation and application (in Chinese), Ph.D. thesis, China Univ. of Geosci., Wuhan.
- Cheng, J. M., C. X. Chen, and M. R. Ji (2004), Determination of aquifer roof extending under the sea from variable-density flow modelling of groundwater response to tidal loading: Case study of the Jahe River Basin, Shandong Province, China, *Hydrogeol. J.*, *12*, 408–423.
- Drogue, C., M. Razark, and P. Krivic (1984), Survey of a coastal karstic aquifer by analysis of the effect of Krast of Slovenia, Yugoslavia, *Environ. Geol. Water Sci.*, *6*, 103–109.
- Ferris, J. G. (1951), Cyclic fluctuations of water level as a basis for determining aquifer transmissibility, *IASH Publ.*, *33*, 148–155.
- Fetter, C. W. (1994), *Applied Hydrogeology*, Prentice-Hall, Upper Saddle River N. J.
- Jacob, C. E. (1940), On the flow of water in an elastic artesian aquifer, *Eos Trans. AGU*, *21*, 547–586.
- Jacob, C. E. (1950), Flow of groundwater, in *Engineering Hydraulics*, edited by H. Rouse, pp. 321–386, John Wiley, Hoboken N.J.
- Jeng, D.-S., L. Li, and D. A. Barry (2002), Analytical solution for tidal propagation in a coupled semi-confined/phreatic coastal aquifer, *Adv. Water Resour.*, *25*, 577–584.
- Jiao, J. J., and Z. Tang (1999), An analytical solution of groundwater response to tidal fluctuation in a leaky confined aquifer, *Water Resour. Res.*, *35*, 747–751.
- Li, G., and C. Chen (1991a), Determining the length of confined aquifer roof extending under the sea by the tidal method, *J. Hydrol.*, *123*, 97–104.
- Li, G., and C. Chen (1991b), The determination of the boundary of confined aquifer extending under the sea by analysis of groundwater level fluctuations (in Chinese), *Earth Sci.*, *16*, 581–589.
- Li, H., and J. J. Jiao (2001a), Tide-induced groundwater fluctuation in a coastal leaky confined aquifer system extending under the sea, *Water Resour. Res.*, *37*, 1165–1171.
- Li, H., and J. J. Jiao (2001b), Analytical studies of groundwater-head fluctuation in a coastal confined aquifer overlain by a leaky layer with storage, *Adv. Water Resour.*, *24*, 565–573.
- Li, H., and J. J. Jiao (2002a), Analytical solutions of tidal groundwater flow in coastal two-aquifer system, *Adv. Water Resour.*, *25*, 417–426.
- Li, H., and J. J. Jiao (2002b), Tidal groundwater level fluctuations in L-shaped leaky coastal aquifer system, *J. Hydrol.*, *268*, 234–243.
- Li, H., and J. J. Jiao (2003), Tide-induced seawater-groundwater circulation in a multi-layered coastal leaky aquifer system, *J. Hydrol.*, *274*, 211–224.
- Li, H., and Q. C. Yang (2000), A least-squares penalty method algorithm for the inverse problems of steady state aquifer models, *Adv. Water Resour.*, *23*, 867–880.
- Li, H., J. J. Jiao, M. Luk, and K. Cheung (2002), Tide-induced groundwater level fluctuation in coastal aquifers bounded by L-shaped coastlines, *Water Resour. Res.*, *38*(3), 1024, doi:10.1029/2001WR000556.
- Li, H., J. J. Jiao, and M. Luk (2004), A falling-pressure method for measuring air permeability of asphalt in laboratory, *J. Hydrol.*, *286*, 69–77.
- Li, L., D. A. Barry, C. Cunningham, F. Stagnitti, and J.-Y. Parlange (2000), A two-dimensional analytical solution of groundwater response to tidal loading in an estuary and ocean, *Adv. Water Resour.*, *23*, 825–833.
- Li, L., D. A. Barry, and D.-S. Jeng (2001), Tidal fluctuations in a leaky confined aquifer: Dynamic effects of an overlying phreatic aquifer, *Water Resour. Res.*, *37*, 1095–1098.

- Maas, C., and W. J. De Lange (1987), On the negative phase shift of groundwater tides near shallow tidal rivers—The Gouderak anomaly, *J. Hydrol.*, *92*, 333–349.
- Sun, H. (1997), A two-dimensional analytical solution of groundwater response to tidal loading in an estuary, *Water Resour. Res.*, *33*, 1429–1435.
- Townley, L. R. (1995), The response of aquifers to periodic forcing, *Adv. Water Resour.*, *18*, 125–146.
- Trefry, M. G. (1999), Periodic forcing in composite aquifers, *Adv. Water Resour.*, *22*, 645–656.
- van der Kamp, G. (1972), Tidal fluctuations in a confined aquifer extending under the sea, *Int. Geol. Cong.*, *24*, 101–106.
- van der Kamp, G. (1973), Periodic flow of groundwater, Ph.D. dissertation, Free Univ., Amsterdam, Netherlands.
- van der Kamp, G., and J. E. Gale (1983), Theory of earth tide and barometric effects in porous formations with compressible grains, *Water Resour. Res.*, *19*, 538–544.

M. C. Boufadel, Department of Civil and Environmental Engineering, Temple University, 1947 North 12th Street, Philadelphia, PA 19122, USA. (boufadel@temple.edu)

J. Cheng, School of Environmental Studies, China University of Geosciences, Wuhan 430074, China. (jmcheng@cug.edu.cn)

G. Li and H. Li, Department of Mathematics, Anshan Normal University, Anshan 114005, China. (liguaniin@yahoo.com.cn; hailong@graduate.hku.hk)